Effect of Operating Parameters and Abrasive Particle Size on Three-Body Abrasion Performance of Alkali-treated Eucalyptus Fiber Reinforced Polyvinyl Chloride Composite

Keping Zhang,* Yongting Cui, and Longpeng Cai

The use of natural fiber polymer composites is being considered in many applications. In the current work, the three-body abrasion performance of an alkali-treated eucalyptus and polyvinyl chloride (PVC) composite was studied at different applied loads (40 to 130 N), sliding velocities (1.86 to 3.73 m/s), sliding distance (up to 4.0 km), and abrasive particle size (0.25 to 0.75 mm). The results showed that the applied load and sliding distance affected three-body abrasion. At lower applied loads and shorter sliding distances, higher specific wear rates (W_s) and more obvious worn surface features were exhibited, while sliding velocity had less of an effect on the wear behavior. The W_s and worn surface roughness increased as abrasive particle size increases, and deeper grooves and higher deformation on the worn surface were found due to the enhanced material loss from the larger particle size abrasive.

Keywords: Eucalyptus; Natural fiber composites; Alkali treatment; Three-body abrasion performance

Contact information: College of Mechanical and Electrical Engineering, Gansu Agricultural University, Lanzhou730070, China; Corresponding author: zhangkp@gsau.edu.cn*

INTRODUCTION

Natural fibers have many advantages such as environmental friendliness, low density, biodegradability, low cost, non-toxicity, and high specific strength; therefore, they offer great potential as reinforcement in polymers for various industrial applications and have a greater impact on socioeconomic development (Chand and Dwivedi 2007; Yousif *et al.* 2010a). There have been many attempts to incorporate natural fibers in polymer-based composites, such as kenaf, jute, bamboo, flax, hemp, sisal, and wood fibers (Yousif *et al.* 2010a,b; Lin *et al.* 2017; Shuhimi *et al.* 2017). The use of natural fiber polymer composites (NFPCs) is increasingly considered in many applications such as sliding panels, linkages, and bearings and bushings. Being cost-effective, they are especially suitable for use in low-cost housing, car interiors, the construction industry, packaging, storage devices, and the automotive industry (El-Tayeb 2008). However, there are some considerations that need to be addressed before NFPCs gain widespread acceptance and confidence for them to be commercially viable; their wear and frictional performance are especially important (Nirmal *et al.* 2012).

As the use of NFPCs for engineering applications subjected to various types of tribological loading conditions has increased, some studies have investigated the tribological behavior of NFPCs. The tribological characteristics of oil palm fiber and polyester composites have been studied, and the effect of operating parameters such as sliding distances, sliding velocities, and applied loads were investigated (Yousif and El-

Tayeb 2007, 2008, 2010). Compared with neat polyester, the specific wear rate (W_s) is lower for oil palm-reinforced polyester composite at various sliding distances, and the W_s decreases at higher applied loads for oil palm-reinforced polyester composite as sliding velocity increases. The wear performance of kenaf fiber reinforced polyurethane composites has been investigated at different applied loads (Chin and Yousif 2009; Singh *et al.* 2011), and there is a slight reduction in the W_s when the applied load increases. When the wear properties of rice husk-reinforced polyvinyl chloride (PVC) composite were studied (Chand *et al*. 2012), the friction and wear values were low for composites compared with neat PVC. The two-body wear behaviors of other NFPCs have been experimentally studied with wheat straw, rice straw, corn straw, sorghum straw (Jiang *et al.* 2017, 2018a,b), bamboo (Nirmal *et al.* 2012), sugarcane (El-Tayeb 2008), cotton (Hashmi *et al.* 2007), and jute (Chand and Dwivedi 2006). Eucalyptus is one of the most widely used genera in global commercial plantation timber industries (Forrester *et al.* 2006), as it is a high quality and high yield tree. Studies have been performed to investigate the mechanical and physical properties of eucalyptus fiber reinforced composites (Espinach *et al.* 2017; Pereira *et al.* 2018). Although a good amount of research is available on tribological properties of NFPCs, there have been few studies on the three-body abrasion behaviors of the eucalyptus fiber reinforced polymer composite.

Previously, the three-body abrasion behaviors of eucalyptus and PVC composite were investigated under fixed operating parameters (Zhang *et al.* 2019). One important method for enhancing the wear resistance of wood-plastic composites is alkali treatment (Alawar *et al.* 2009; Phuong *et al.* 2010; Saha *et al.* 2010; Yousif *et al.* 2010b). The 5% NaOH alkali-treated eucalyptus and PVC composites had a noticeably improved three-body abrasion resistance (Zhang *et al.* 2019). The purpose of this study is to explore the effect of operating parameters such as applied load, sliding velocity, sliding distance, and the abrasive particle size on three-body abrasion behaviors of alkali-treated eucalyptus fiber reinforced PVC composites for potential engineering applications.

EXPERIMENTAL

Materials

Eucalyptus (*Eucalyptus robusta* Smith) was purchased from Guangxi Fenglin Wood Industry Co., Ltd., Guangxi, China. The density was 0.611 g/cm^3. Its chemical composition included fibrin (42.31%), half-fibrin (16.65%), lignin (24.38%), and ash (4.38%). The SG-5 PVC was purchased from Tianjin Tongxingguo Trading Co., Ltd., Tianjin, China. The 400A maleic anhydride graft coupling agent and 603 non-toxic Ca/Zn composite stabilizer were purchased from Guangzhou Yinghong Chemical Co., Ltd., Guangzhou, China. The H-108 PE (polyethylene) wax was purchased from WujiangMeiqi Plastic Material Co., Ltd., Suzhou, China.

The sand abrasives used in this work were sourced from the Yellow River in Lanzhou, China. The sand was washed, air-dried, and filtered with mesh screens to obtain particle sizes of 0.25 mm, 0.50 mm, and 0.75 mm.

The air-dried eucalyptus was initially crushed, subsequently ground, and finally filtered with a 100-mesh screen (149 μm pore size). Selected eucalyptus fibers were soaked in 5% NaOH concentrations at 100 °C for 1 h (solid-liquid ratio = 1:2). The treated fibers were separated from the liquid by filtration and washed with deionized water until the rinsed solution became neutral. The rinsed fibers were dried at 90 °C for 16 h in a DHG-

9055A electrical thermostatic drum-wind drying oven (Shanghai Yiheng Scientific Instrument Co., Ltd., Shanghai, China), then cooled to room temperature in the oven, obtaining a moisture content of less than 3%.

Based on the pre-experiment data, the alkali-treated eucalyptus fiber, PVC, coupling agent, stabilizer, and PE wax (mass ratio = 100:100:3:8:5, respectively) were mixed in a SYH-5 3D linkage mixer (Changzhou Feima Drying Equipment Co., Ltd., Changzhou, China). The compound was then placed into a SY-6216 inter-meshing twin-screw extruder (Shiyan Precision Instruments Co., Ltd., Guangdong, China). During the extrusion, the temperature profiles from the hopper to die zone were controlled at 150, 155, 160, and 165 °C, and the rotational speed of the screw was 20 rpm. The extruded samples had a width and thickness of 25.5 mm and 6 mm, respectively, and the density of the samples was 2.355 g/cm^3. The lengths of the NFPCs were verified and controlled by the extrusion period. The solidified samples were cut to a length of 57 mm with a hand saw for further wear tests.

Three-body Wear Test

The three-body wear test was carried out using a rubber-rimmed wheel three-body sand abrasive wear tester shown in Fig. 1a (MLS-225; Zhangjiakou Taihua Machine Co., Ltd., Zhangjiakou, China) at room temperature (20 ± 1 °C). The schematic diagram of the tester is shown in Fig. 1b. The Shore hardness of the rimmed rubber was A-70 degree and the circumference of the rubber wheel was 0.559 m. During the test, the specimen (6 × 25.5 × 57 mm^3) was pressed against the rimming rubber wheel by the applied load. The maximum value of the applied load for the tester is 225 N. The rotational speed of the rubber wheel can be controlled and adjusted continuously between 0 and 500 r/min using a frequency converter, corresponding to between 0 and 4.66 m/s in linear velocity.

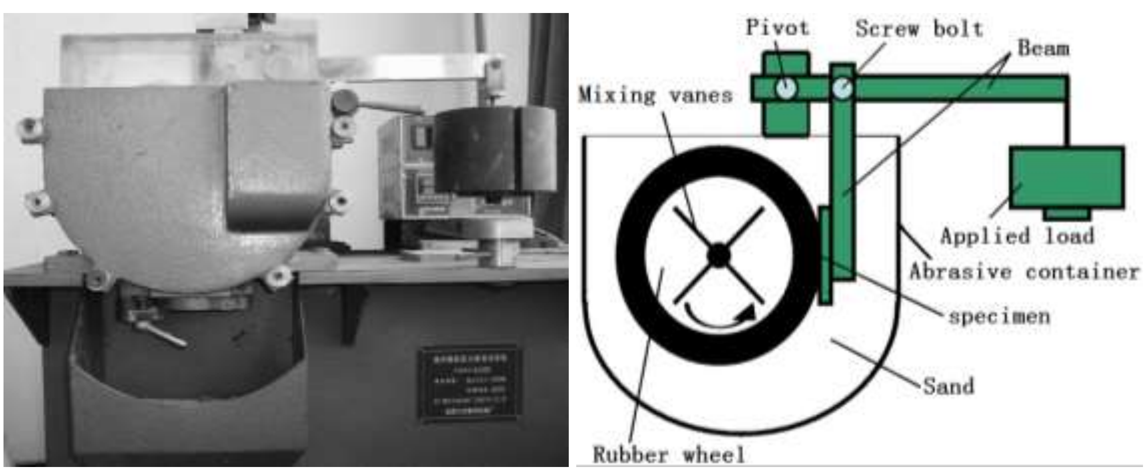

a) b)

Fig. 1. (a) Three-body sand abrasive wear tester and (b) Schematic diagram of the tester

In this work, the tests were conducted at different applied loads (40 to 130 N), sliding velocities (1.86 to 3.73 m/s with a corresponding rotational speed of 200 to 400 r/min), sliding distances (up to 4.0 km), and were subjected to different sizes of abrasive sand particles (0.25 to 0.75 mm of particle size), which were placed in the abrasive container. The abrasive container was filled up with sand particles in each test. A summary of the operating parameters and particle sizes is presented in Table 1. For each test, a new specimen was used, and the surfaces of the specimen were cleaned with absolute ethanol and air-dried before and after each test. Each test was repeated on at least three independent specimens.

Table 1. Parameters for the Wear Test

Test parameter	Unit	Value
Applied load	N	40, 70, 100, 130
Sliding velocity	$m \cdot s^{-1}$	1.86, 2.80, 3.73
Sliding distance	km	1.0, 2.0, 3.0, 4.0
Sand particle size	mm	0.25, 0.50, 0.75

The specific wear rate (W_s) was calculated by determining the weight loss and density of the test specimen and using Eq. 1 (Jeamtrakull *et al.* 2012),

$$W_S = \frac{\Delta M}{LF\rho} \quad (1)$$

where ΔM is the weight loss (mg), L is the sliding distance (m), F is the applied load (N), and ρ is the specimen density (g/cm^3). The weight loss of the test specimen was measured using an AUY 220 electronic analytical balance (Shimazu (China) International Trade, Co., Ltd., Tianjin, China) with an accuracy of 0.1 mg. The density of the specimen was measured using a TD-120 high precision touch screen plastic density tester (Taizhou Tiande Instrument Equipment Co., Ltd., Taizhou, China).

The roughness of the wear track was measured before and after the test using an SRA profile and roughness tester (Shanghai Optical Instrument Factory, Shanghai. China), the test direction parallel to the sliding in each measurement. The average roughness of five measurements in different regions of the eucalyptus and PVC composite specimens before the test was about 0.22 μm (Fig. 2).

Fig. 2. Sample of the roughness profile of the eucalyptus and PVC composite specimen surface

Morphological analysis of the worn surfaces was performed by a Hitachi-S3400N scanning electron microscopy (SEM) (Hitachi Ltd., Tokyo, Japan). Prior to the SEM analysis, the worn surfaces of the specimens were coated with gold by an MSP-1S Magnetron sputter coater (Vacuum Device Inc., Tokyo, Japan).

RESULTS AND DISCUSSION

Effect of Applied Load and Sliding Distance

The effect of applied load and sliding distance on three-body abrasion behaviors was tested by varying the applied load and sliding distance, while keeping the sliding velocity and abrasive particle size constant. Figure 3 shows the effect of the applied load and sliding distance on the W_s of alkali-treated eucalyptus and PVC composite at different applied loads and sliding distances, while the sliding velocity was 2.8 m/s and sand particle size was 0.5 mm.

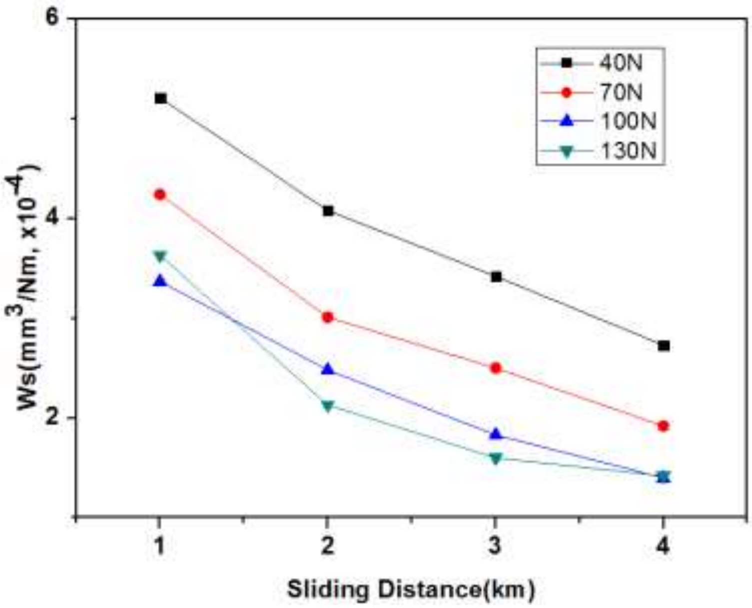

Fig. 3. Variation of the W_s with sliding distance at different applied loads, sliding velocity 2.8 m/s and sand particle size 0.5 mm

Figure 3 indicates that the W_s decreased gradually at all applied loads as the sliding distance increased, and the decrease rate of W_s slowed down slightly after 2 km of sliding distance. This is because more eucalyptus fibers were exposed to the wear surface as the wear was continued, and these exposed eucalyptus fibers enhanced the wear resistance of the matrix material, which can be further evidenced in the morphology investigation of the worn surfaces.

When the applied load was changed in the range of 40 to 100 N, the W_s decreased clearly as the load increased, with higher W_s being observed at lower loads. This is because the relative motion between the sand particles and the surface of the composite specimen in the three-body wear process slows down with the increased applied load, and the wear loss caused by periodic fatigue decreased. However, when the load was increased from 100 to 130 N, the decrease of W_s gradually lessened, and there was even an increased W_s in some sliding distance areas, which could be due to the increase of wear loss caused by multiple plastic deformation under high applied load.

Due to the material removal during three-body wear test, the profile of the composite specimen worn surface was altered. Roughness profiles for the worn surfaces of the alkali-treated eucalyptus and PVC composite at different applied loads are shown in Fig. 4, while the sliding distance was 4 km, the sliding velocity was 2.8 m/s, and sand particle size was 0.5 mm.

Compared with the original surface roughness of 0.22 µm, the surface roughness of the composite specimen increased after tests with all applied loads, which could be attributed to the wear loss of surface material during the test. The roughness of the worn surface decreased as applied load increased, which is similar to the change rate of W_s with applied load. The material removal of wear surface decreased with increased applied loads, resulting in the lower roughness.

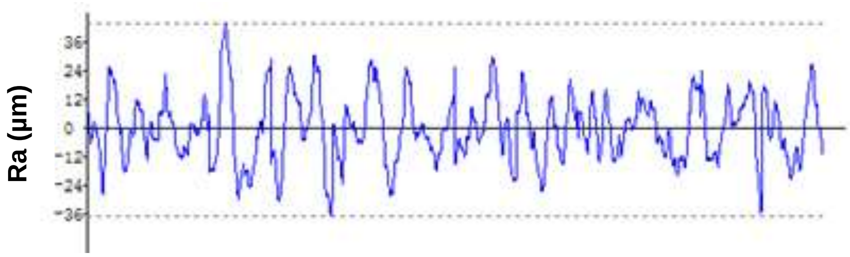

a) Applied load of 40 N, Ra is 10.905 µm

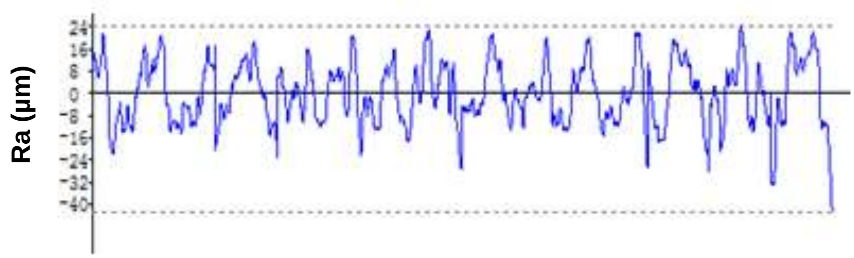

b) Applied load of 70 N, Ra is 9.278 µm

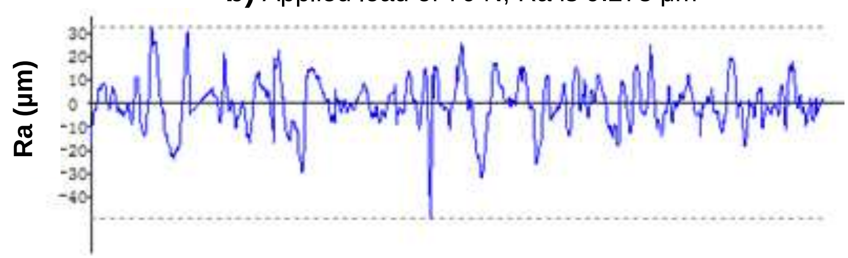

c) Applied load of 100 N, Ra is 7.509 µm

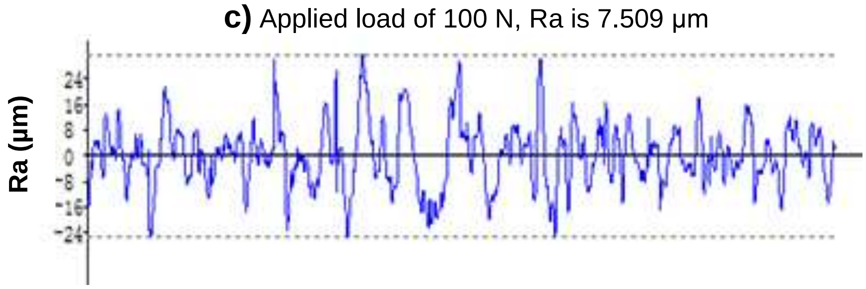

d) Applied load of 130 N, Ra is 7.479 µm

Fig. 4. Roughness profile samples for the worn surfaces of the eucalyptus and PVC composite specimens at different applied loads with sliding distance 4 km, sliding velocity 2.80 m/s and sand particle size 0.5 mm

Figure 5 contains SEM micrographs of the composite worn surface under 40, 70, 100, and 130 N applied loads, respectively, while the sliding distance, sliding velocity, and sand particle size are constant. Fig. 5(e-g) is the SEM observation under 1, 2 and 3 km sliding distances, respectively, with fixed applied load, sliding velocity, and sand particle size.

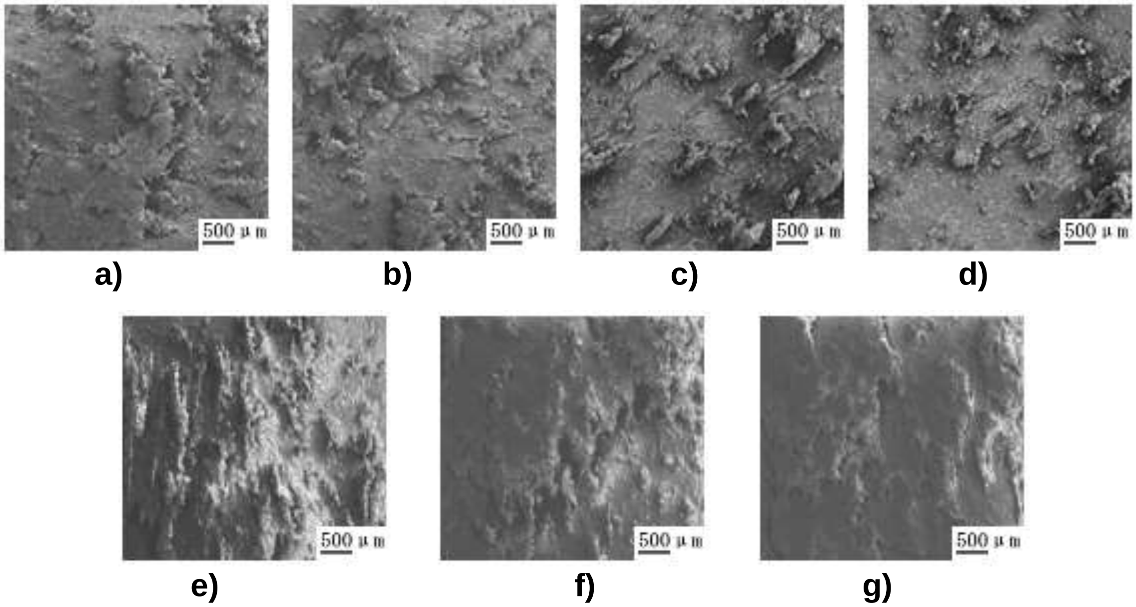

Fig. 5. SEM micrograph samples of worn surface at different applied loads (a, b, c, and d while sliding distance 4 km): a) Applied load of 40 N; b) Applied load of 70 N; c) Applied load of 100 N ; d) Applied load of 130 N. Different sliding distances (e, f, and g, while applied load 100 N), sliding velocity 2.8 m/s, and sand particle size 0.5 mm: e) Sliding distance of 1 km; f) Sliding distance of 2 km; g) Sliding distance of 3 km.

Obvious abrasive wear features, such as furrows and pits, were apparent on all of the worn surface micrographs. With increased applied load (Figs. 5a to 5d), the furrows and pits became shallower and smoother, which indicates decreased three-body abrasion. The effect of the sliding distance on worn surface can be seen from Figs. 5e to 5g, some of the eucalyptus fibers were exposed after 1 km wear, while most of them were still covered by matrix material (Fig. 5e). As the wear continued to 3 km, more exposed eucalyptus fibers were visible, as shown in Fig. 5g. The exposed fibers could form a strong layer against the sand abrasive which protects the polyester region and reduces the mass loss of the composite (Chang *et al.* 2018), which is verified by the fact of gradual decrease of the W_s with increased sliding distance.

Effect of Sliding Velocity

The W_s variation with sliding velocity of alkali-treated eucalyptus and PVC composite is presented in Fig. 6, with a sliding distance of 3 km and sand particle size of 0.5 mm.

There was a slight increase in W_s for all applied loads when the sliding velocity increased from 1.86 to 2.80 $m \cdot s^{-1}$. More sand particles were brought in contact with the specimen surface as the sliding velocity increased, and the three-body abrasion is aggravated by those extra particles, resulting in more material removal. The W_s increased continuously when the sliding velocity increased at lower applied loads (40 and 70 N). For higher applied loads (100 and 130 N), there was no obvious change in W_s when sliding velocity increased from 2.80 to 3.73 $m \cdot s^{-1}$, due to the prevention of particle sliding along the composite surface under higher applied loads.

The average roughness value of the specimen worn surface at different sliding velocities is shown in Fig. 7, with the applied load 100 N, sliding distance 3 km, and sand particle size 0.5 mm.

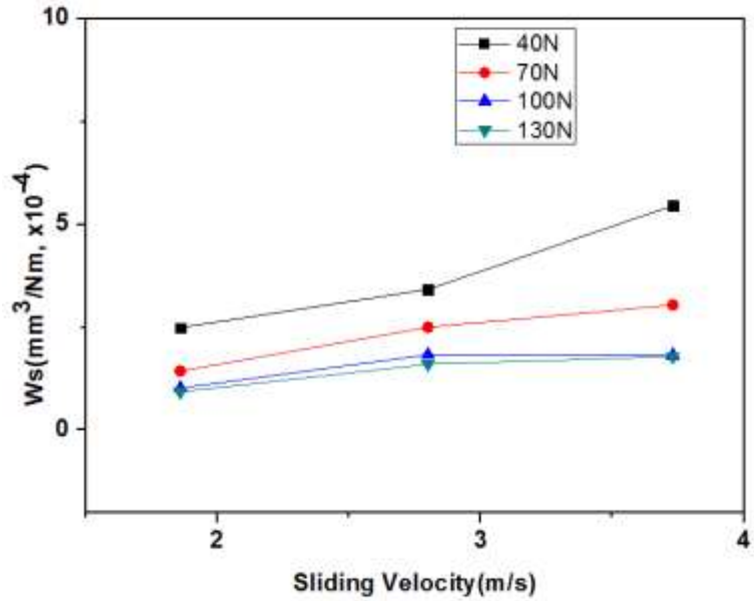

Fig. 6. Variation of the W_s with sliding velocity at different applied loads with sliding distance 3 km and sand particle size 0.5 mm

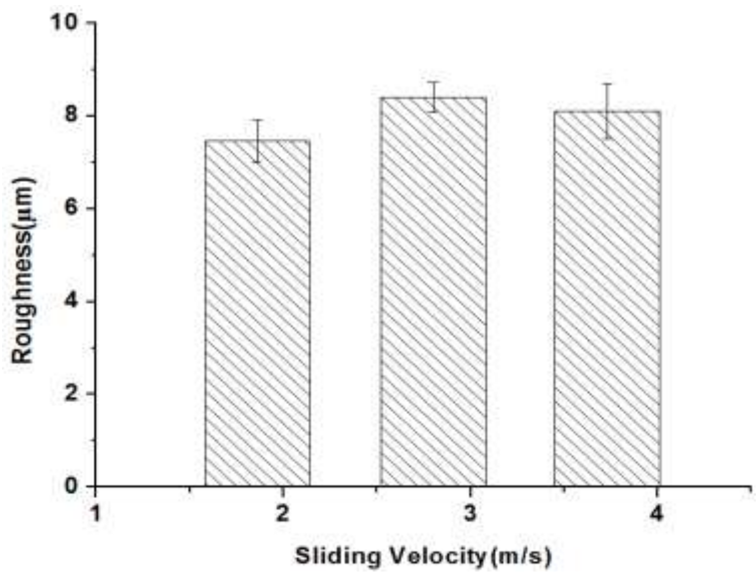

Fig. 7. Worn surface roughness at different sliding velocities with applied load 100N, sliding distance 3 km, and sand particle size 0.5 mm

There was a slight increase of surface roughness when the sliding velocity increased from 1.86 to 2.80 $m \cdot s^{-1}$ (Fig. 7), while a slight decrease in surface roughness was found as sliding velocity increased from 2.80 to 3.73 m/s. In general, sliding velocity had an insignificant effect on the worn surface roughness of alkali-treated eucalyptus and PVC composite.

The effect of sliding velocity on the characteristics of the worn surface is shown in Fig. 8 (a, b, and c) at 1.86, 2.80 and 3.73 m/s with applied load 100 N, sliding distance 3 km, and sand particle size 0.5 mm. Furrows, pits and exposed eucalyptus fibers were observed in all SEM micrographs in Fig. 8. Furrows and pits were not apparent at a sliding velocity of 1.86 m/s compared with the others. Furthermore, some of the exposed fibers were mixed with the deformed polyester debris as shown in Fig. 8c, and a similar phenomenon was noted previously (Yousif and El-Tayeb 2007). This could be the reason that W_s and surface roughness decreased when the sliding velocity was 3.73 m/s.

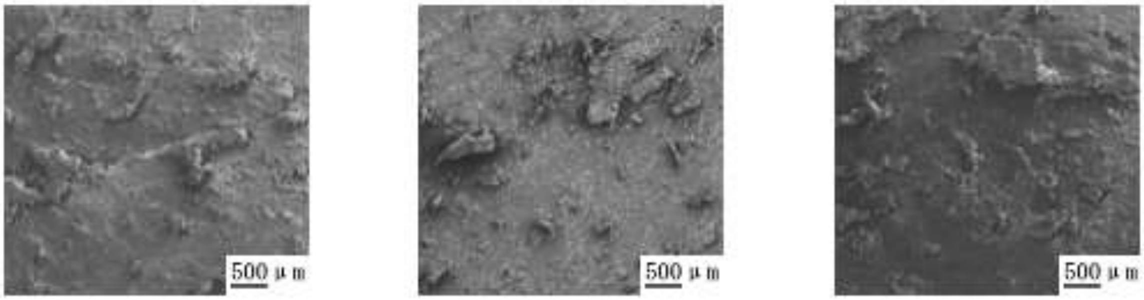

a) b) c)

Fig. 8. SEM micrographs of the worn surface at different sliding velocities with applied load 100 N, sliding distance 3 km, and sand particle size 0.5 mm: a) Sliding velocity of 1.86 m/s; b) Sliding velocity of 2.80 m/s; c) Sliding velocity of 3.73 m/s

Effect of Abrasive Particle Size

The W_s of alkali-treated eucalyptus and PVC composite subjected to different applied loads against three particle size levels of sand abrasive is shown in Fig. 9. In general, there was a similar change trend of W_s with particle size increasing under all applied loads. The W_s increased with the increased size of sand particle at all applied loads, which is consistent with previous reports (Bijwe *et al.* 2002; Yousif *et al.* 2010c).

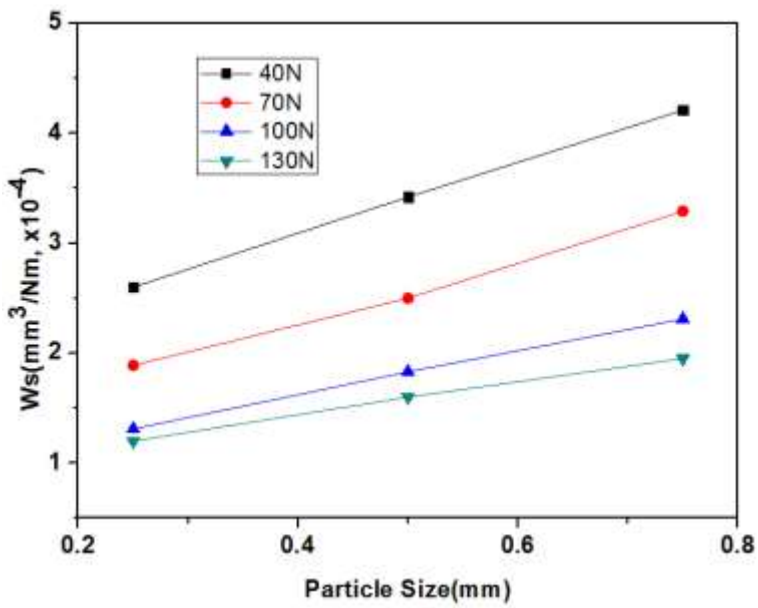

Fig. 9. Variation of the W_s with sand particle size at different applied loads, sliding distance 3 km and sliding velocity 2.8 m/s

The roughness profile of the specimen surface after wear tests with different sand particle size are shown in Fig. 10 under an applied load of 100 N, sliding velocity of 2.80 m/s, and sliding distance of 3 km. Compared with the original eucalyptus and PVC composite specimen surface roughness of 0.22 µm, the surface roughness of the specimen was highly increased after the wear test with all of the three sand particle abrasives. The average roughness values of the worn surface at the three sand abrasive sizes were 6.83, 8.57, and 11.24 µm, respectively. The roughness value increased as the sand particle size increased, which could be due to the more obvious wear features under larger sand abrasive.

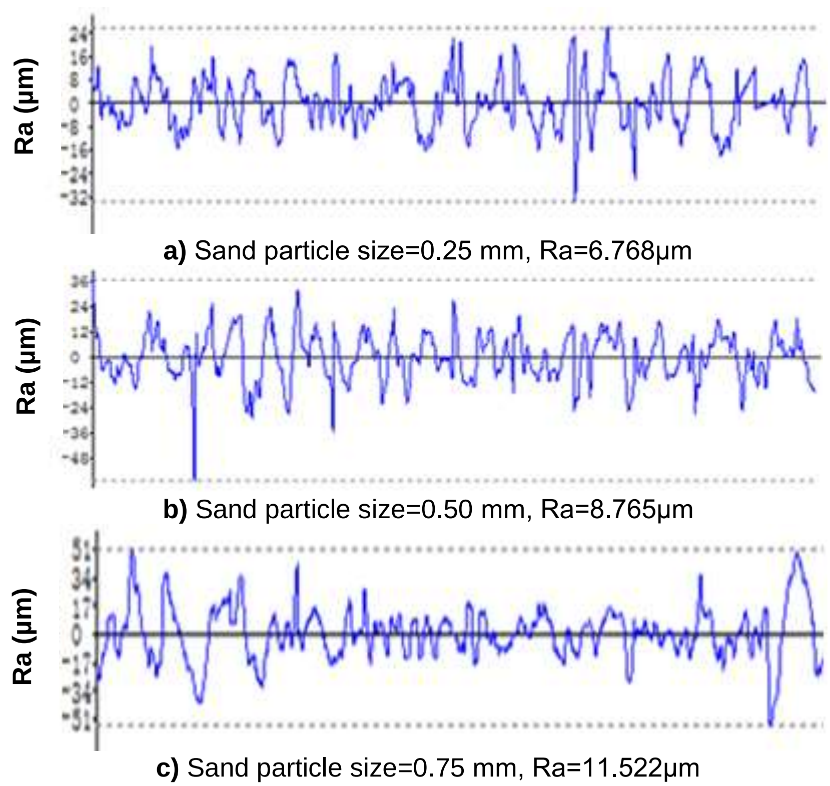

Fig. 10. Roughness profile of the specimen worn surface at different sand particle size with applied loads 100 N, sliding velocity 2.80 m/s, and sliding distance 3 km

Figure 11 shows the SEM micrographs of the worn surface of the composite under 0.25, 0.50, and 0.75 mm particle size abrasives. The wear behavior was aggravated with increased abrasive particle size, which is proved by deeper grooves and higher deformation on the worn surface as shown in Figs. 11a to 11b. The same trend has also been observed for W_s and surface roughness with increased abrasive particle size. This may be due to the deeper penetration with a larger particle size abrasive, which enhances the material removal from the composite surface (Yousif *et al*. 2010c).

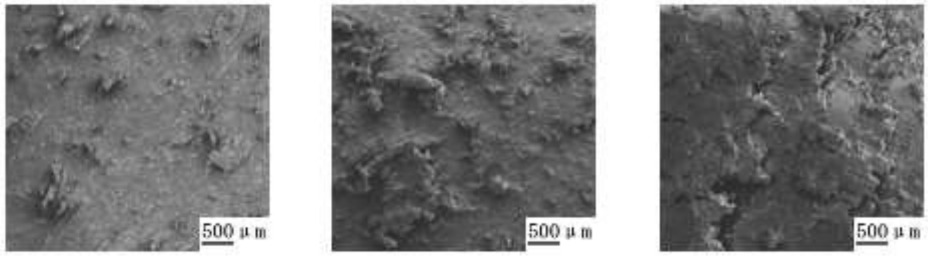

a) b) c)

Fig. 11. SEM micrographs of worn surface at different particle size, applied loads 100 N, sliding velocity 2.80 m/s, and sliding distance 3 km: a) Particle size=0.25 mm; b) Particle size=0.50 mm; c) Particle size=0.75 mm

CONCLUSIONS

1. The applied load and sliding distance affect three-body abrasion significantly; higher specific wear rate (W_s) and more obvious worn surface features were apparent at lower applied loads and shorter sliding distances. On the other hand, sliding velocity had less of an effect on the wear behavior at the range of 1.83 to 3.73 m/s.
2. With increases in abrasive particle size between 0.25 and 0.75 mm, the W_s and worn surface roughness increased; deeper grooves and higher deformation were found on the worn surface under larger particle sizes due to enhancement of the material loss from the composite surface.

ACKNOWLEDGEMENTS

This work was supported by the Discipline Construction Fund Project of Gansu Agricultural University, Grant No. GAU-XKJS-2018-191 and the Fund for Young Supervisor of Gansu Agricultural University, Grant No. GAU-QNDS-201711.

REFERENCES CITED

Alawar, A., Hamed, A. M., and Al-Kaabi, K. (2009). "Characterization of treated date palm tree fiber as composite reinforcement," *Composites Part B: Engineering* 40(7), 601-606. DOI: 10.1016/j.compositesb.2009.04.018

Bijwe, J., Indumathi, J., and Ghosh, A. K. (2002) "On the abrasive wear behaviour of fabric reinforced polyetherimide composites," *Wear* 253, 768-777. DOI: 10.1016/s0043-1648(02)00169-2

Chand, N., and Dwivedi, U. K. (2006). "Effect of coupling agent on abrasive wear behaviour of chopped jute fibre-reinforced polypropylene composites," *Wear* 261(10), 1057-1063. DOI: 10.1016/j.wear.2006.01.039

Chand, N., and Dwivedi, U. K. (2007). "High stress abrasive wear study in bamboo," *Journal of Materials Processing Technology* 183(2-3), 155-159. DOI: 10.1016/j.jmatprotec.2006.09.036

Chand, N., Fahim, M., Sharma, P., and Bapat, M. N. (2012). "Influence of foaming agent on wear and mechanical properties of surface modified rice husk filled

polyvinylchloride," *Wear* 278-279, 83-86. DOI: 10.1016/j.wear.2012.01.002
Chang, B. P., Chan, W. H., Zamri, M. H., Akil, H. M., and Chuah, H. G. (2018). "Investigating the effects of operational factors on wear properties of heat-treated pultruded kenaf fiber-reinforced polyester composites using taguchi method," *Journal of Natural Fibers* 16, 702-717. DOI: 10.1080/15440478.2018.1432001
El-Tayeb, N. S. M. (2008). "A study on the potential of sugarcane fibers/polyester composite for tribological applications," *Wear* 265(1–2), 223-235. DOI: 10.1016/j.wear.2007.10.006
Espinach, F. X., Granda, L. A., Tarres, Q., Duran, J., Palmer, P. F., and Mutje, P. (2017). "Mechanical and micromechanical tensile strength of eucalyptus bleached fibers reinforced polyoxymethylene composites," *Composites Part B: Engineering* 116, 333-339. DOI: 10.1016/j.compositesb.2016.10.073
Forrester, D. I., Bauhus, J., Cowie, A. L., and Vanclay, J. K. (2006). "Mixed-species plantations of Eucalyptus with nitrogen-fixing trees: A review," *Forest Ecology and Management* 233(2-3), 211-230. DOI: 10.1016/j.foreco.2006.05.012
Hashmi, S. A. R., Dwivedi, U. K., and Chand, N. (2007). "Graphite modified cotton fibre reinforced polyester composites under sliding wear conditions," *Wear* 262(11-12), 1426-1432. DOI: 10.1016/j.wear.2007.01.014
Jeamtrakull, S., Kositchaiyong, A., Markpin, T., Rosarpitak, V., and Sombatsompop, N. (2012). "Effects of wood constituents and content, and glass fiber reinforcement on wear behavior of wood/PVC composites," *Composites Part B: Engineering* 43(7), 2721-2729. DOI: 10.1016/j.compositesb.2012.04.031
Jiang, L., He, C., Fu, J., and Chen, D. (2017). "Wear behavior of straw fiber-reinforced polyvinyl chloride composites under simulated acid rain conditions," *Polymer Testing* 62, 373-381. DOI: 10.1016/j.polymertesting.2017.07.028
Jiang, L., He, C., Fu, J., and Li, X. (2018a). "Wear behavior of alkali-treated sorghum straw fiber reinforced polyvinyl chloride composites in corrosive water conditions," *BioResources* 13(2), 3362-3376. DOI: 10.15376/biores.13.2.3362-3376
Jiang, L., He, C., Fu, J., and Wang, L. (2018b). "Serviceability analysis of wood-plastic composites impregnated with paraffin-based pickering emulsions in simulated sea water-acid rain conditions," *Polymer Testing* 70, 73-80. DOI: 10.1016/j.polymertesting.2018.06.031
Lin, X., Zhang, Z., Tan, S., Wang, F., Song Y., Wang Q., Charles, U., and Pittman, J. (2017). "In line wood plastic composite pyrolyses and HZSM-5 conversion of the pyrolysis vapors," *Energy Conversion and Management* 141, 206-215. DOI: 10.1016/j.enconman.2016.07.071
Nirmal, U., Hashim, J., and Low, K. O. (2012). "Adhesive wear and frictional performance of bamboo fibres reinforced epoxy composite," *Tribology International* 47, 122-133. DOI: 10.1016/j.triboint.2011.10.012
Saha, P., Manna, S., Chowdhury, S. R., Sen, R., Roy, D., and Adhikari, B. (2010). "Enhancement of tensile strength of lignocellulosic jute fibers by alkali-steam treatment," *Bioresource Technology* 101(9), 3182-3187. DOI: 10.1016/j.biortech.2009.12.010
Shuhimi, F., Abdollah, M. F. B., Kalam M. A., Masjuki H. H., Mustafa, A., Kamal, E., and Amiruddin, H. (2017). "Effect of operating parameters and chemical treatment on the tribological performance of natural fiber composites: A review," *Particulate Science and Technology* 35:5, 512-524. DOI: 10.1080/02726351.2015.1119226
Singh, N., Yousif, B. F., and Rilling, D. (2011). "Tribological characteristics of

sustainable fibre-reinforced thermoplastic composites under wet adhesive wear," *Tribology Transactions* 54 (5), 736-748. DOI: 10.1080/10402004.2011.597544
Pereira, T. G. T., Mendes, J. F., Oliveira, J. E., Marconcini, J. M., and Mendes, F. R. (2018). "Effect of reinforcement percentage of eucalyptus fibers on physico-mechanical properties of composite hand lay-up with polyester thermosetting matrix," *Journal of Natural Fibers* 16, 806-816. DOI: 10.1080/15440478.2018.1439426
Yousif, B. F., and El-Tayeb, N. S. M. (2007). "The effect of oil palm fibres as reinforcement on tribological performance of polyester composite," *Surface Review Lett*ers 14(6), 1095-1102. DOI: 10.1142/s0218625x07010561
Yousif, B. F., and El-Tayeb, N. S. M. (2008). "Adhesive wear performance of T-OPRP and UT-OPRP composites," *Tribology Letters* 32 (3), 199-208. DOI: 10.1007/s11249-008-9381-7
Yousif, B. F., and El-Tayeb, N. S. M. (2010). "Wet adhesive wear characteristics of untreated oil palm fibre-reinforced polyester and treated oil palm fibre-reinforced polyester composites using the pin-on-disc and block-on-ring techniques," *Proceedings of the Institution of Mechanical Engineers, Part J: Journal of Engineering Tribology* 224 (2), 123-131. DOI: 10.1243/13506501jet655
Yousif, B. F., Lau, S. T. W., and Mcwilliam, S. (2010a). "Polyester composite based on betel nut fibre for tribological applications," *Tribology International* 43(1), 503-511. DOI: 10.1016/j.triboint.2009.08.006
Yousif, B. F., Leong, O. B., Ong, L. K., and Jye, W. K. (2010b). "The effect of treatment on tribo-performance of CFRP composites," *Recent Patents on Materials Science* 2(1), 67-74. DOI: 10.2174/1874465610902010067
Yousif, B. F., Nirmal, U., and Wong, K. J. (2010c). "Three-body abrasion on wear and frictional performance of treated betelnut fibre reinforced epoxy (T-BFRE) composite," *Materials and Design* 31(9), 4514-4521. DOI: 10.1016/j.matdes.2010.04.008
Zhang, K., Cui, Y., and Yan, W. (2019). "Thermal and three-body abrasion behaviors of alkali-treated eucalyptus fiber reinforced polyvinyl chloride composites," *BioResources* 14(1), 1229-1240. DOI: 10.15376/biores.14.1.1229-1240

Article submitted: November 26, 2019; Peer review completed: December 31, 2019; Revised version received and accepted: January 3, 2020; Published: January 7, 2020.
DOI: 10.15376/biores.15.1.1298-1310